Journal of Engineering Science and Technology
Vol. 14, No. 5 (2019) 2792 - 2807

CHARACTERIZATION OF OIL PALM EMPTY FRUIT BUNCH (EFB) BIOCHAR ACTIVATED WITH POTASSIUM HYDROXIDE UNDER DIFFERENT PYROLYSIS TEMPERATURE

MOHD HAIRY AZWAN BIN MOHD BAKHTIAR[1],
NORAZLINA BINTI ABU SARI[2], ADZMI BIN YAACOB2,
MOHD FADIL BIN MOHD YUNUS[3], KHAIROL BIN ISMAIL[3]

[1,3]Malaysian Agriculture and Research and Development Institute (MARDI),
MARDI Headquarters, 43400 Serdang, Selangor.
[2]Faculty of Plantation and Agrotechnology, Universiti Teknologi MARA,
404500 Shah Alam, Selangor
*Corresponding Author: mhairyazwan@mardi.gov.my

Abstract

Malaysia is among the top oil palm producers and exporters in the world. In consequence, this industry creates a huge amount of empty fruit bunch (EFB) as an agriculture by-product from the processing line. In order to convert this waste biomass into high value-added products, biochar from oil palm EFB was activated by using KOH under low, medium and high activation temperature. (400 ºC, 600 ºC and 800 ºC). The physico-chemical characteristics of activated EFB biochars were evaluated by using proximate and ultimate analysis, Brunauer-Emmet-Teller (BET) surface area, surface morphology using Scanning Electron Microscope (SEM) and Fourier Transform Infrared (FTIR) spectrometer. The results of activated EFB biochar that produced at low and medium temperature (400 ºC and 600 ºC) had shown high in yield, well developed pores and enriched with oxygen containing functional groups (O-H and C-O). In contrast, biochar that activated with high activation temperature (800 ºC) produced more total and fixed carbon, high BET surface area, total pore volume and micropore volume as well as aromatic nature.

Keywords: Activated biochar, Characterization, Empty fruit bunch, Potassium hydroxide, Surface area, Surface functional groups.

1. Introduction

Biochar is a carbonaceous material produced from the conversion process of biomass with the absent or limited supply of oxygen [1]. Recently, biochar has been used as a universal adsorbent material in various applications such as soil and water treatment, gas purification, health and pharmaceutical, gold purification and sewage treatment [2-4]. However, biochar has limited ability and capacity to adsorb contaminants at high concentration. Thus, the conventional biochar needs further improvements in order to increase its adsorption ability and capacity.

The improvement of biochar using various method such as chemical activation, physical activation, impregnation with mineral sorbents, and magnetic modifications has been received interest among researchers. According to a review work by Li et al. [5], the activation process of biochar increases their porous structure, surface area and alter their functional groups, which had further increased their sorption capacity.

Malaysia is known as the second largest palm oil producer in the world and among the biggest exporter of upstream and downstream of oil palm products [6]. In consequence, this industry dispersed a huge amount of agriculture wastes such as empty fruit bunch (EFB), mesocarp fibre and palm kernel shell that were disposed by 452 palm oil mills in Malaysia, throughout the year [7]. According to Abdul et al. [8], approximately 15 million tons of EFB are generated annually and this amount is expected to increase because of high global demand on oil palm products. Since EFB has high carbon content, rich in lignin and available locally and abundantly, it has the potential as a precursor for the production of activated biochar.

In recent years, there has been tremendous interest in production of biochar and activated carbon using agriculture wastes [9-12]. However, it is crucial to understand and to choose the most suitable biochar for further application since the physicochemical properties of biochar mainly depend on feedstock and production conditions, where the pyrolysis temperature is the most influenced. Even though there are a number of studies [13, 14] regarding the using of various activation method in the production of activated EFB, but as far as the author are aware, there is no information on the preparation of activated EFB biochar using KOH as activation agent, under different activation temperatures. Therefore, the aims of this study were to produce and characterize activated EFB biochar based on physicochemical properties, morphology, BET surface area and FTIR functional groups and to determine the optimum temperature of activated EFB biochar for being used as heavy metals adsorbent.

2. Materials and Method

2.1. Preparation of raw EFB and activated EFB biochar

Raw EFB biomass was collected from Kempas Oil Palm Mill, Sime Darby Bhd located in Merlimau, Malacca, Malaysia. Biomass sample then was air-dried for one week and oven dried at 70 ºC for 48 h to eliminate excessive moisture. The dried sample was chopped at about 4-6 mm of particle size and kept in a container for the activation steps.

The EFB sample undergo two steps of the KOH activation process according to Abechi et al. [15] with some modifications. The EFB sample was carbonized in a muffle furnace at 350 ºC for 2 h to develop the initial porosity of biochar. Then, the carbonization sample (20 g) was mixed with 200 cm^3 KOH solution at impregnation

ratio of 1:1 (KOH pallet: Sample). The mixture was stirred continuously and being heated for 2 h at 85 ºC and speed of 6 rpm. The sample was filtered and dried overnight at 120 ºC in an oven. After that, the sample was activated at 400 ºC in a furnace for 45 min. The 45 min of retention time was fixed in this study since it is recognized as the optimum retention time to produce activated carbon [15]. Next, the activated sample was washed several times with 0.1 M HCl and distilled water in order to remove any remaining KOH component and organic residual in the sample. Lastly, the activated sample was dried in an oven at 102 ºC for 24 h. The same steps were repeated for the next sample that activated with 600 and 800 ºC of activation temperature. The dried sample was kept in a desiccator until further analysis.

The KOH impregnation and pyrolysis temperature play an important role to determine the yield of activated EFB biochar. According to the study by Claoston et al. [16], EFB biochar did not fully carbonized at 300 ºC of pyrolysis temperature. Meanwhile at high temperature (above 800 ºC), there was an extreme reduction in the most of biochar yields [17-19]. Hence, the activation temperature of 400, 600 and 800 ºC were chosen in this study, since it involved the variety of low, medium and high temperature for the most of biochar production, in order to obtain optimum biochar yield, besides having good physicochemical properties.

2.2. Activated EFB biochar yield

The yield of activated EFB biochar sample was measured to determine the recovery of produced char after being pyrolysed under different temperatures and the yield of activated EFB biochar was calculated based on the following Eq. (1):

$$Yield\ (\%) = \frac{M2}{M1}\ x\ 100 \tag{1}$$

where, *M1* is the initial dry weight (g) of char precursor and *M2* is the dry weight of final activated EFB biochar (g).

2.3. Characterization of activated EFB biochar

2.3.1. Proximate and ultimate analysis

Proximate analysis was carried out to study the relative moisture, volatile matters, ash and fixed carbon contents in the samples. The analysis was carried out by following Standard Test Method for Chemical Analysis of Wood Charcoal, ASTM D1762-84 [20]. Ultimate analysis was conducted to determine carbon, nitrogen, hydrogen and oxygen content of samples by using CHNS Analyser from Thermo Scientific™. The percentage of oxygen was determined by difference. All the samples were analysed in triplicated.

2.3.2. BET surface area

The Brunauer, Emmett and Teller (BET) surface area, pore size and surface area distributions, micropore volume and surface area of activated EFB biochar were measured by nitrogen adsorption at 77 K using 3 Flex Surface Characterization Analyser (Micromeritics Instrument Corporation) after being degassed at 300 °C in an inert condition for 24 h.

2.3.3. Surface morphology

The surface morphology of activated EFB biochar was observed under JEOL, JSM-6010 PLUS/LV Scanning Electron Microscope in order to obtain the pores structure.

2.3.4. FTIR surface functional groups

The surface functional groups of activated EFB biochar was measured by using pellet press Kbr disc method through Fourier Transform Infrared (FTIR) Spectrometer (Perkin Elmer Corporation, Norwalk, CT, USA), where the spectra were recorded from 4000 to 500 cm^{-1}.

3. Results and Discussion

A series of activated biochars were prepared from EFB as a precursor using KOH as activation agent under 400 (AB400), 600 (AB600) and 800 ºC (AB800) of activation temperature. The effects of different activation temperatures on yield, proximate and ultimate analysis, surface area and surface functional groups were also studied and discussed as follows:

3.1. Effects of KOH activation under various activation temperatures on activated EFB biochar yield

As can be seen from Fig. 1, the yield of activated EFB biochar was gradually diminished as activation temperature increased. The rate of carbonization of biochar was enhanced with increasing activation temperature from 400 to 800 ºC. This could be attributed due to the thermal degradation of organic and inorganic material that was released in the form of volatile components, which resulting in a higher carbon burn off, thus contributing to the greater weight loss in the carbon containing fraction [21]. In addition, Khalil et al. [22] reported that the increase in activation temperature also would increase the KOH-carbon reactions, thus accelerated the oxidation process on the outer surface of carbon atoms that led to the formation of pores and reduced carbon yield.

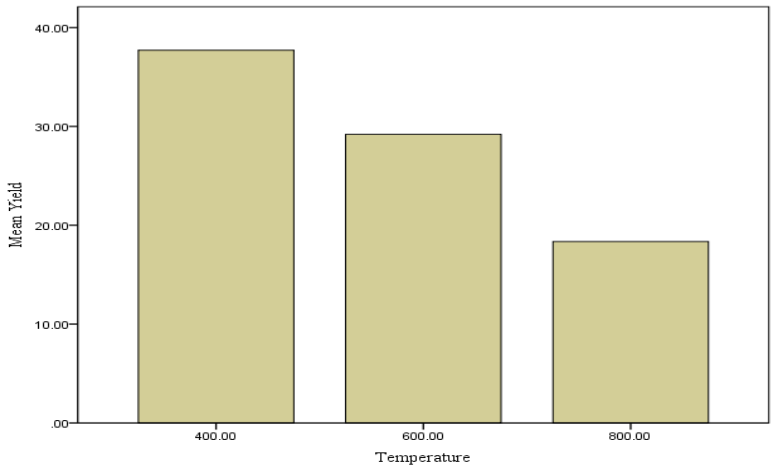

Fig. 1. Yield of activated EFB biochar under 400, 600 and 800 ºC of activation temperature.

3.2. Effects of KOH activation under various temperatures on physicochemical properties of activated EFB biochar

Table 1 shows the results of proximate and ultimate analysis results for activated EFB biochars that have been chemically activated using KOH at 400, 600 and 800 ºC of activation temperature. Proximate analysis was performed to determine the moisture, volatile matter, ash and fixed carbon content of the produced chars.

As can be seen from proximate analysis results in Table 1, moisture content was decreased from 3.74% to 0.98% as the increasing in activation temperature. Moisture content is defined as a loss of water from the initial weight of materials. As the activation temperature increase from 400 to 800 ºC, the water contents of biochar were evaporated, which resulted in a significant reduction in moisture contents. According to Aziz et al. [23], the excessive moisture content will fill up the empty space between pore spaces of biochar and cause the biochar to undergo sudden crack as a result of structures fragility.

Meanwhile the volatile matter contents were experienced a reduction from 27.6% to 11.4% as the activation temperature increased. Since these were two step of biochar activation process, the high volatile matter contents at low activation temperature was probably due to the presence of lignin in EFB biomass that partially withstand a primary thermal degradation at 400 ºC during carbonization stage [24]. During the activation process, the secondary thermal degradation continued to reduce the degree of devolatilisation thus reducing the volatile matters content of the produced chars [25].

In contrast, the ash content steadily increased as temperature increased due to the high thermal degradation of lignocellulosic material and mineral elements during the activation process that has contributed to the accumulation of ash content in biochar [26].

The fixed carbon content also increased with the increasing of activation temperature from 62.9% to 78.92%. When EFB biomass was pyrolysed, labile organic matter in the EFB was destroyed aggressively from 400 to 800 ºC while fixed carbon was more persistence as higher temperature needed to burn off the more stable form of carbon [27]. The high fixed carbon content is important because it will determine the high biochar stability and recalcitrant towards physical, chemical and biological degradation [28]. Besides that, Kan et al. [29] summarized that the criteria for determining good quality of biochar or activated carbon are through the high fixed carbon content and low moisture, volatile matters and ash content.

Meanwhile, the ultimate analysis indicated chemical composition of the produced char that mainly consists of carbon, hydrogen, oxygen and nitrogen. Total carbon values increased from 40.08 to 60.04 upon the increased of activation temperature. This evidence shows that the degree of carbonization was accelerated at high activation temperature [30]. In contrast, the total H, N and O were decreased with the increasing of activation temperature from 4.44 to 2.45, 0.717 to 0.361 and 51.16 to 32.35 respectively. Meanwhile, pyrolysis temperatures do not influence the S content in produced char. The greater losses of the total H and O content at high temperature were assumed as a consequence from the dehydration and decarboxylation reactions by cleavage and breakage due to the weak bonds within

biochar structure [31]. In addition, the loss of N in the increasing of activation temperature was probably due to the ignition loss during the activation process [32].

The degree of carbonization of biochar may also be described from the H/C molar ratio. As shown in Table 1, the H/C molar ratio was decreased with the increasing of activation temperature. The H/C of 0.49 for AB800 suggested that the degree of carbonization and aromaticity are high at this temperature [33]. In contrast, the higher value of H/C ratio obtained at 1.32 and 0.72, indicated that the slow thermal decomposition of lignocellulosic materials such as cellulose, hemicellulose and lignin, begin at lower to medium temperature (400 and 600 ºC) as compared to higher activation temperature.

According to Batista et al. [34], the polar groups on biochar surface, acts as water adsorption centers and aids in the formation of water clusters on the surface of biochar. Therefore, the molar O/C ratio can be used to determine the hydrophilicity on the surface of biochar. As stated in Table 1, the O/C molar ratio was decreased with the increasing of activation temperature. AB400 was more hydrophilic as it contains higher O/C ratio (0.96) than those AB600 (0.53) and AB800 (0.40). It also indicated that AB400 contains higher polar group content compare to others. In contrast, biochar activated under higher temperature (AB800) resulted in low O/C ratio and became less hydrophilic.

Table 1. Proximate and ultimate analysis of activated EFB biochars.

Analysis	Parameter	AB 400	AB 600	AB 800
Proximate	Moisture content (%)	3.74±0.09	2.05±0.12	0.98±0.01
	Volatile matter (%)	27.60±0.46	23.23±0.20	11.44±0.00
	Ash content (%)	5.76±0.18	7.05±0.07	8.66±0.20
	Fixed carbon (%)	62.90±10.0	67.67±1.2	78.92±1.25
Ultimate	Total N (%)	0.717±0.02	0.559±0.03	0.361±0.01
	Total C (%)	40.08±1.0	54.94±1.3	60.04±0.3
	Total H (%)	4.44±0.3	3.30±0.16	2.45±0.03
	Total S (%)	3.60±0.13	2.36±0.08	4.79±0.4
	Total 0 (%)	51.16±0.51	38.80±1.52	32.35±0.85
	H/C molar ratio	1.32	0.72	0.49
	O/C molar ratio	0.96	0.53	0.4

Fixed Carbon % was estimated by different =100-(%Moisture+%Volatile+%Ash)
Total O % was estimated by different =100-(%N+%C+%H+%S)
H/C atomic ratio of hydrogen to carbon. O/C: atomic ratio of oxygen to carbon.
The values are mean ± standard error.

3.3. Effects of various activation temperature on BET surface area of activated EFB biochar

The surface area and pore properties of activated EFB biochar were presented in the Table 2. As can be seen, BET surface area, total pore volume and micropore volume was obviously increased with the increasing of activation temperature. Activated EFB biochar that produced at 800 ºC showed the highest BET surface

area of 920.67 m^2g^{-1} while the lowest BET surface area was recorded at 90.65 m^2g^{-1}, which obtained from 400 ºC of activation temperature. Total pore volume and micropore volume were also increased from 0.02 to 0.24 cm^3g^{-1} and 0.007 to 0.17 cm^3g^{-1} when the temperature was increased from 400 to 800 ºC. Nevertheless, the average pore diameter was decreased from 83.66 to 20.86 Å when temperature was further increased up to 800 ºC.

Similar trends in BET surface area and porosity were observed for the production of activated biochar at the increasing of temperature [35, 36]. From the results of this study, the increasing of BET surface area, total pore volume and micropore volume were significantly influenced by the activation temperatures and reaction between KOH and carbonized sample [37]. Initially, the thermal degradation of raw EFB at 350 ºC during the carbonization process has released a significant amount of volatile matters (mostly non-carbon elements such as H, N and O), which induced the development of initial pore structure [38]. Normally, the initial pore structure in this sample has low porosity with structure disordered. The further increasing of temperature led to the destruction of the wall between two adjacent pores, thus increasing the surface area of produced char [39]. Besides, the increasing of activation temperature also would increase the KOH-carbon reactions, resulting in increasing devolatilisation, which would then enhance and widening the existing pores and created new porosities [40]. This is in agreement with this study where total pore volume and micropore volume were also increased from 0.02 to 0.24 cm^3/g and 0.007 to 0.17 cm^3/g when the temperature increased from 400 to 800 ºC.

The KOH acts as a catalyst to accelerate the pore development. Furthermore, the increased in total pore volume and micropore volume as a result from intercalation of potassium ion into the carbon matrix that widens the existing pores and creates new porous structures that led to the formation of micropores, mesopores or macropores [41]. Meanwhile, the further extension of activation temperature from 400 to 800 ºC significantly reduced the pore diameter from 83.66 to 20.86 A. This was reported by Mohamad et al. [42] that as temperature increased, the diameter of the sample would decrease, which can cause the development of micropore volume.

Table 2. BET surface area, total pore volume, micropore volume and average pore diameter of activated EFB biochar under various activation temperatures.

Sample	BET surface area (m^2/g)	Total pore volume (cm^3/g)	Micropore volume (cm^3/g)	Average pore diameter (A)
AB 400	90.65	0.02	0.007	83.66
AB 600	580.47	0.1	0.06	25.08
AB 800	920.67	0.24	0.17	20.86

3.4. Effects of KOH activation under various activation temperature on organic functional groups of activated EFB biochar

Figure 2 shows the FTIR functional groups for the activated EFB biochar produced under different activation temperatures. It can be seen that the complex spectra bands have been developed upon the activation process and the trend of all spectra bands is quite similar to each other's. The number of functional groups was increased at activation temperature 400 and 600, but it was decreased at higher activation temperature of 800.

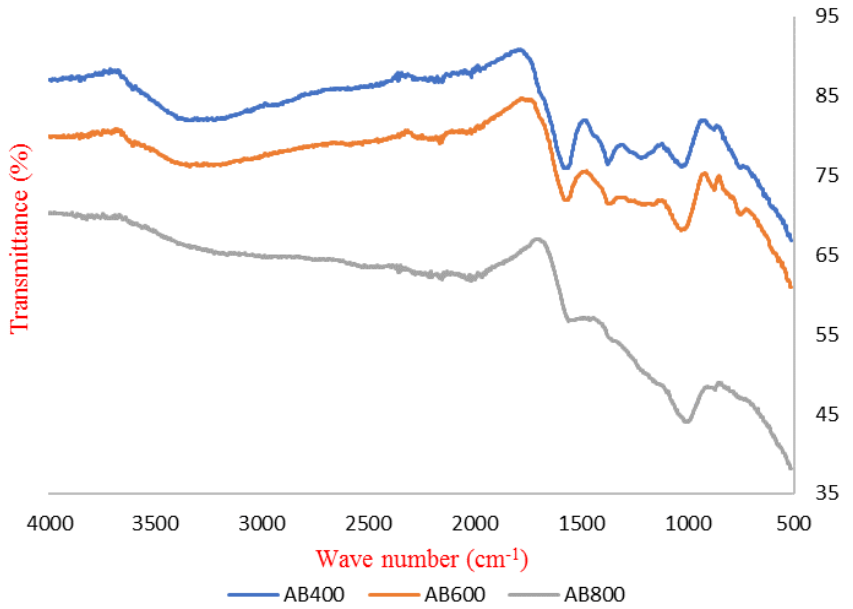

Fig. 2. FTIR spectra of activated EFB biochar with KOH activation at 400, 600 and 800 °C.

Table 3 summarized the functional groups obtained from the FTIR spectra for each produced chars. The broad adsorption peak detected at 3339.14 cm^{-1} (AB400), 3336.02 and 2516.63 cm^{-1} (AB600), as well as 3197.6514 cm^{-1} (AB800), was attributed to the O-H stretching vibration of hydroxyl functional groups. As expected, the domination of hydroxyl group in each activated EFB biochar was believed due to moisture, cellulose and hemicellulose component in EFB [43]. The peak observed at 2156.55, 2207.43 and 2016.80 cm^{-1} for AB400, AB600 and AB800 were identified as thiocyanate (S-C ≡ N), alkyne (C = C) and isothiocyanate (N = C = S) group.

The adsorption bands at 1574.36, 1569.71 and 1558.4 cm^{-1} for all produced chars were probably due to the cyclic alkene group with C = C stretching of aromatic ring. An alkane stretching C-H band was found at 1373.6 and 1370.82 cm^{-1} for AB400 and AB600 respectively. On the other hand, the aliphatic alkyl aryl ether compound vibrations were found at 1218.42, 1206.69 and 1010.99 cm^{-1} at all activation temperatures. The vinyl ether from the C-O stretching vibration was

identified at 1026.94 and 1030.41 cm^{-1} in AB400 and AB600. The peaks observed at 874.52, 872.57 and 751.42 cm^{-1} in AB400 and AB600 were probably due to the presence of aromatic C-H group in the activated EFB biochar.

Based on this study, the different activation temperatures have significantly influenced by the number of functional groups of the produced chars. Results obtained from this study have revealed that EFB biochar activated at lower and medium activation temperature (400 and 600 ºC) produced higher number of oxygen containing (O-H and C-O) functional groups compared to those at 800 ºC.

This could be attributed to the slow dehydration process in EFB at lower temperature. This finding was in agreement with previous studies on biochar and activated carbon [44, 45]. Furthermore, KOH enhanced the formation of O-H functional groups on the activated EFB biochars surface [46]. According to Jamari and Howse [47], the reduction in the number of functional groups at higher activation temperature (800 ºC) was believed due to the process of dehydration and deoxygenation of lignocellulosic material (cellulose, hemicellulose and lignin) that diminished the aliphatic structures and followed by the formation of aromatic structure. This could be explained by the presents of aromatics and aromatic C-O group in this study, which was believed to have come from lignin in the EFB biomass [48].

Table 3. Summary of functional groups for activated EFB biochars based on adsorption peak from FTIR spectra.

Sample	Wave number(cm^{-1})	Functional group	Bond
AB 400	3339.14	Alcohol	O-H
	2156.55	Thiocyanate	S-C ≡ N
	1574.36	Cyclic alkene	C = C
	1373.60	Alkane	C-H
	1218.42	Alkyl aryl ether	C-O
	1026.94	Vinyl ether	C-O
	874.52	1,2,4-trisubstituted	C-H
AB 600	3336.02	Alcohol	O-H
	2516.63	Carboxylic acid	O-H
	2207.43	Alkyne	C ≡ C
	1569.71	Cyclic alkene	C = C
	1370.82	Alkane	C-H
	1206.69	Alkyl aryl ether	C-O
	1030.41	Vinyl ether	C-O
	872.57	1,2,4-trisubstituted	C-H
	751.42	1,2-monosubstituted benzene derivative	C-H
AB 800	3197.65	Alcohol	O-H
	2016.80	Isothiocyanate	N = C=S
	1558.40	Cyclic alkene	C = C
	1010.99	Alkyl aryl ether	C-O

3.5. Effects of activation temperature on surface morphology of activated EFB biochar

The changes in surface morphology of EFB biochar after activated with KOH under different temperatures are presented in Figs. 3(a) to (f). The SEM analysis was conducted to study the morphology of biochar surface. In order to get clear pictures on the surface changes and the pore development at different pyrolysis temperatures, the images were taken on the surface and tip of biochar, at different resolution (from 200 to 1,000 magnifications).

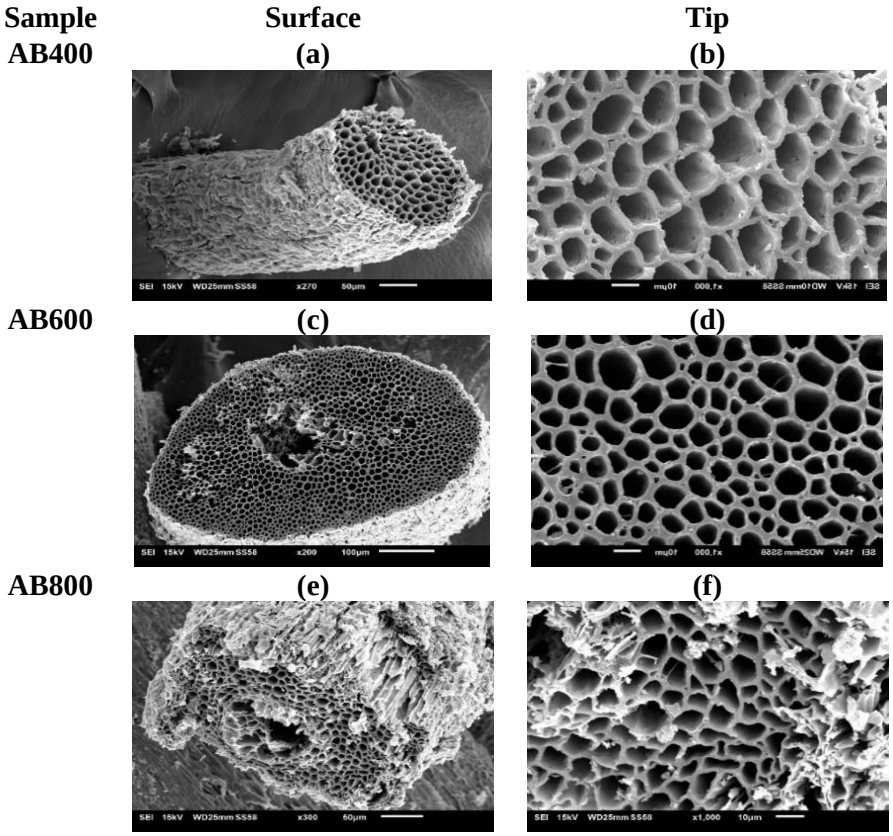

Fig. 3. SEM images of activated EFB biochar treated with KOH under different activation temperature; 400 ºC (a) and (b), 600 ºC (c) and (d), and 800 ºC (e) and (f).

Generally, there are obviously differences among the produced chars, in term of surface texture and pores size distribution, with increasing pyrolysis temperature. The pore size for AB400, AB600 and AB800 shows that the pores diameter ranging between 7.3 to 1.7µm, which indicated, that mesopores were successfully developed for all biochar. In view of result obtained, biochar that pyrolysed at 400 ºC exhibit rough surface texture and well-developed pores with honeycomb like shape, Figs. 3(a) and (b). At 600 ºC, the surface texture did not much differ as at 400 ºC, but the inner core seems started to diminish.

As the pyrolyse temperature was further increased to 800 ºC, the outer surface of biochar was started to fracture and collapse, while the inner core is continuing to diminish. This finding has revealed that the EFB biochar cannot withstand at high temperature (800 ºC) as the surface structure and inner core was easily fragile and finally diminished. This result obtained is in agreement with Claoston et al. [16], where the cracks and shrinkages were observed on the surface of biochar as a result of high pyrolysis temperature.

Apart from pyrolysis temperature, KOH was also believed to have a significant effect on the morphology of activated EFB biochar. Komnitsas and Zaharaki [49] have revealed that the development of microporous structure on the surface of pistachio shell biochar after treated with KOH and $FeCl_3$, which is in agreement with this study where the microporous structure was also observed (Fig. 3). In addition, XX also found that biochar activated with KOH also produces smooth surface texture and well-developed porosity as compared to non-activated biochar.

4. Conclusion

Three activated EFB biochar with different properties were obtained from this investigation. The findings from this study revealed that KOH activation under different activation temperature had contributed a greater impact on the physicochemical properties of the produced chars. Activated EFB biochar produced at low (AB400) to medium temperature (AB600) contributed to the high yield, well developed pores structure, contains more aliphatic properties and enriched with oxygen containing surface functional groups such as O-H and C-O.

This character will provide an excellent medium for ion exchange capacity during the adsorption process. Meanwhile, activated EFB biochar produced at high activation temperature (AB800) experienced on low yield, more fixed and total carbon, high BET surface area as well as more aromatic nature and less oxygen containing functional groups due to the dehydration and deoxygenation of biomass. In addition, the BET surface area for AB600 and AB800 were within the range 400-1400 m^2/g of commercial activated carbon [50]. In order to evaluate the performance of all these activated EFB biochar as heavy metals adsorbent, future work such as adsorption or incubation study are urgently needed.

Acknowledgement

The authors would like to acknowledge to Faculty of Plantation and Agrotechnology, Universiti Teknologi MARA (UiTM), Research Management Institute (RMI), UiTM and Ministry of Higher Education Malaysia. This research was partially supported by the Internal Research Acculturation Grant Scheme [600-RMI/IRAGS 5/3 (49/2015)].

Nomenclatures

AB	Activated biochar
ASTM	American Society for Testing and Materials
BET	Brunauer-Emmet-Teller
CHNSO	Carbon Hydrogen Nitrogen Sulfur Oxygen
EFB	Empty fruit bunch

FTIR	Fourier Transform Infrared
HCL	Hydrochloric acid
KOH	Potassium hydroxide
Kbr	Potassium bromate
MPOB	Malaysian Palm Oil Board

References

1. Lehmann, J.; and Joseph, S. (2015). *Biochar for environmental management: Science, technology and implementation* (2nd ed.). Abingdon, United Kingdom: Routledge.
2. Solanki, A.; and Boyer, T.H. (2017). Pharmaceutical removal in synthetic human urine using biochar. *Environmental Science: Water Research and Technology*, 3(3), 553-565.
3. Dalahmeh, S.; Ahrens, L.; Gros, M.; Wiberg, K.; and Pell, M. (2018). Potential of biochar filters for onsite sewage treatment: Adsorption and biological degradation of pharmaceuticals in laboratory filters with active, inactive and no biofilm. *Science of the Total Environment*, 612, 192-201.
4. Uchimiya, M.; Pignatello, J.J.; White, J.C.; Hu, S.-L.; and Ferreira, P.J. (2017). Surface interactions between gold nanoparticles and biochar. *Scientific Reports*, 7(1), 1-9.
5. Li, H.; Dong, X.; da Silva, E.B.; de Oliveira, L.M.; Chen, Y.; and Ma, L.Q. (2017). Mechanisms of metal sorption by biochars: Biochar characteristics and modifications. *Chemosphere*, 178, 466-478.
6. Alam, A.S.A.F.; Er, A.C.; and Begum, H. (2015). Malaysian oil palm industry: Prospect and problem. *Journal of Food Agriculture and Environment*, 13(22), 143-148.
7. Malaysian Palm Oil Board (MPOB). (2019). Number and capacities of palm oil sectors in operation as at August 2019. Retrieved October 7, 2019, from http://bepi.mpob.gov.my/index.php/en/statistics/sectoral-status/370-sectoral-status-2019/917-number-a-capacities-of-palm-oil-sectors-2019.html.
8. Abdul, P.M.; Jahim, J.M.; Harun, S.; Markom, M.; Lutpi, N.A.; Hassan, O.; Balan, V.; Dale, B.E.; and Nor, M.T.M. (2016). Effects of changes in chemical and structural characteristic of ammonia fibre expansion (AFEX) pretreated oil palm empty fruit bunch fibre on enzymatic saccharification and fermentability for biohydrogen. *Bioresource Technology*, 211, 200-208.
9. Wahi, R.; Aziz, S.M.A.; Hamdan, S.; and Ngaini, Z. (2015). Biochar production from agricultural wastes via low-temperature microwave carbonization. *Proceedings of the IEEE International RF and Microwave Conference (RFM)*. Kuching, Malaysia, 4 pages.
10. El-Naggar, A.H.; Alzhrani, A.K.R.; Ahmad, M.; Usman, A.R.A.; Mohan, D.; Ok, Y.S.; and Al-Wabel, M.I. (2016). Preparation of activated and non-activated carbon from Conocarpus pruning waste as low-cost adsorbent for removal of heavy metal ions from aqueous solution. *BioResources*, 11(1), 1092-1107.

11. Shamsuddin, M.S.; Yusoff, N.R.N.; and Sulaiman, M.A. (2016). Synthesis and characterization of activated carbon produced from kenaf core fiber using H3PO4 activation. *Procedia Chemistry*, 19, 558-565.
12. Zhang, J.; Liu, J.; and Liu, R. (2015). Effects of pyrolysis temperature and heating time on biochar obtained from the pyrolysis of straw and lignosulfonate. *Bioresource Technology*, 176, 288-291.
13. Wahyuningsih, P.; Yusri, N.; and Hamdani. (2016). Characterization of activated carbon prepared from oil palm empty fruit bunch by chemical activation using sulphuric acid (H2SO4). *Proceedings of the International Conference on Engineering and Science for Research and Development (ICESReD)*. Banda Acheh, Indonesia, 239-244.
14. Hameed, B.H.; Tan, I.A.W.; and Ahmad, A.L. (2009). Preparation of oil palm empty fruit bunch-based activated carbon for removal of 2, 4, 6-trichlorophenol: Optimization using response surface methodology. *Journal of Hazardous Materials*, 164(2-3), 1316-1324.
15. Abechi S.E.; Gimba, C.E.; Uzairu, A.; and Dallatu, Y.A. (2013). Preparation and characterization of activated carbon from palm kernel shell by chemical activation. *Research Journal of Chemical Sciences*, 3(7), 54-61.
16. Claoston, N.; Samsuri, A.W.; Ahmad Husni, M.; and Amran, M.S.M. (2014). Effects of pyrolysis temperature on the physicochemical properties of empty fruit bunch and rice husk biochars. *Waste Management and Research: The Journal of the International Solid Wastes and Public Cleansing Association* (ISWA), 32(4), 331-339.
17. Wasim, A.A.; and Khan, M.N. (2016). Physicochemical effect of activation temperature on the sorption properties of pine shell activated carbon. *Water Science and Technology*, 75(5), 1158-1168.
18. Xu, P.; Sun, C.-X.; Ye, X.-Z.; Xiao, W.-D.; Zhang, Q.; and Wang, Q. (2016). The effect of biochar and crop straws on heavy metal bioavailability and plant accumulation in a Cd and Pb polluted soil. *Ecotoxicology and Environmental Safety*, 132, 94-100.
19. Yashim, M.M.; Razali, N.; Saadon, N.; and Rahman, N.A. (2016). Effect of activation temperature on properties of activated carbon prepared from oil palm kernel shell (OPKS). *ARPN Journal of Engineering and Applied Sciences*, 11(10), 6389-6392.
20. ASTM International. (2007). Standard test method for chemical analysis of wood charcoal. *ASTM D1762-84*.
21. Osman, N.B.; Shamsuddin, N.; and Uemura, Y. (2016). Activated carbon of oil palm empty fruit bunch (EFB); core and shaggy. *Procedia Engineering*, 148, 758-764.
22. Khalil, H.P.S.A.; Firoozian, P.; Bakare, I.O.; Akil, H.M.; and Noor, A.M. (2010). Exploring biomass-based carbon black as filler in epoxy composites: Flexural and thermal properties. *Materials and Design*, 31(7), 3419-3425.
23. Aziz, N.S.A.; Nor, M.A.M.; Manaf, S.F.A.; and Hamzah, F. (2015). Suitability of biochar produced from biomass waste as soil amendment. *Procedia - Social and Behavioral Sciences*, 195, 2457-2465.

24. Jindo, K.; Mizumoto, H.; Sawada, Y.; Sanchez-Monedero, M.A.; and Sonoki, T. (2014). Physical and chemical characterization of biochars derived from different agricultural residues. *Biogeosciences*, 11(23), 6613-6621.
25. Mopoung, S.; Moonsri, P.; Palas, W.; and Khumpai, S. (2015). Characterization and properties of activated carbon prepared from tamarind seeds by KOH activation for Fe (III) adsorption from aqueous solution. *The Scientific World Journal*, 2015, Article ID 415961, 9 pages.
26. Conz, R.F.; Abbruzzini, T.F.; de Andrade, C.A.; Milori, D.M.B.P; and Cerri, C.E.P. (2017). Effect of pyrolysis temperature and feedstock type on agricultural properties and stability of biochars. *Agricultural Sciences*, 8, 914-933.
27. Xie, T.; Sadasivam, B.Y.; Reddy, K.R.; Wang, C.; and Spokas, K. (2015). Review of the effects of biochar amendment on soil properties and carbon sequestration. *Journal of Hazardous, Toxic, and Radioactive Waste*, 20(1), 14 pages.
28. Yargicoglu, E.N.; Sadasivam, B.Y.; Reddy, K.R.; and Spokas, K. (2015). Physical and chemical characterization of waste wood derived biochars. *Waste Management*, 36, 256-268.
29. Kan, T.; Strezov, V.; and Evans, T.J. (2016). Lignocellulosic biomass pyrolysis: A review of product properties and effects of pyrolysis parameters. *Renewable and Sustainable Energy Reviews*, 57, 1126-1140.
30. Chen, Y.; Yang, H.; Wang, X.; Zhang, S.; and Chen, H. (2012). Biomass based pyrolytic polygeneration system on cotton stalk pyrolysis: Influence of temperature. *Bioresource Technology*, 107, 411-418.
31. Xin, S.; Yang, H.; Chen, Y.; Yang, M.; Chen, L.; Wang, X.; and Chen, H. (2015). Chemical structure evolution of char during the pyrolysis of cellulose. *Journal of Analytical and Applied Pyrolysis*, 116, 263-271.
32. Rafiq, M.K.; Bachmann, R.T.; Rafiq, M.T.; Shang, Z.; Joseph, S.; and Long, R. (2016). Influence of pyrolysis temperature on physico-chemical properties of corn stover (zea mays l): Biochar and feasibility for carbon capture and energy balance. *PLoS ONE,* 11(6), 17 pages.
33. Chen, B.; Zhou, D.; and Zhu, L. (2008). Transitional adsorption and partition of nonpolar and polar aromatic contaminants by biochars of pine needles with different pyrolytic temperatures. *Environmental Science and Technology*, 42(14), 5137-5143.
34. Batista, E.M.C.C.; Shultz, J.; Matos, T.T.S.; Fornari, M.R.; Ferreira, T.M.; Szpoganicz, B.; de Freitas, R.A.; and Mangrich, A.S. (2018). Effect of surface and porosity of biochar on water holding capacity aiming indirectly at preservation of the Amazon biome. *Scientific Reports*, 8(1), 9 pages.
35. Kawano, T.; Kubota, M.; Onyango, M.S.; Watanabe, F.; and Matsuda, H. (2008). Preparation of activated carbon from petroleum coke by KOH chemical activation for adsorption heat pump. *Applied Thermal Engineering*, 28(8-9), 865-871.
36. Saka, C. (2012). BET, TG-DTG, FT-IR, SEM, iodine number analysis and preparation of activated carbon from acorn shell by chemical activation with ZnCl2. *Journal of Analytical and Applied Pyrolysis*, 95, 21-24.

37. Yahya, M.A.; Zanariah C.W.; Ngah, C.W.; Hashim, M.A.; and Al-Qodah, Z. (2015). Preparation of activated carbon from desiccated coconut residue by chemical activation with NaOH. *Journal of Materials Science Research*, 5(1), 24-31.

38. Lee, C.L.; H'ng, P.S.; Paridah, T.; Chin, K.L.; Khoo, P.S.; Nazrin, R.A.R.; Asyikin, S.N.; and Maminski, M. (2016). Effect of reaction time and temperature on the properties of carbon black made from palm kernel and coconut shell. *Asian Journal of Scientific Research*, 10(1), 24-23.

39. Kumar, A.; and Jena, H.M. (2016). Preparation and characterization of high surface area activated carbon from fox nut (Euryale ferox) shell by chemical activation with H_3PO_4. *Results in Physics*, 6, 651-658.

40. Tan, I.A.W.; Ahmad, A.L.; and Hameed, B.H. (2008). Preparation of activated carbon from coconut husk: Optimization study on removal of 2, 4, 6-trichlorophenol using response surface methodology. *Journal of Hazardous Materials*, 153(1-2), 709-717.

41. Zhang, X. (2015). *Synthesis, characterization of novel porous carbon materials and their application in CO_2 capture.* Ph.D. Thesis. University of Alberta, Edmonton, Canada.

42. Mohamed, A.R.; Mohammadi, M.; and Darzi, G.N. (2010). Preparation of carbon molecular sieve from lignocellulosic biomass: A review. *Renewable Sustainable Energy Review*, 14(6), 1591-1599.

43. Wafti, N.S.A.; Lau, H.L.N.; Loh, S.K.; Aziz, A.A.; Rahman, Z.A.; and May, C.Y. (2017). Activated carbon from oil palm biomass as potential adsorbent for palm oil mill effluent treatment. *Journal of Oil Palm Research*, 29(2), 278-290.

44. Liu, P.; Liu, W.-J.; Jiang, H.; Chen, J.-J.; Li, W.-W.; and Yu, H.-Q. (2012). Modification of bio-char derived from fast pyrolysis of biomass and its application in removal of tetracycline from aqueous solution. *Bioresource Technology*, 121, 235-240.

45. Rajapaksha, A.U.; Chen, S.S.; Tsang, D.C.W.; Zhang, M.; Vithanage, M.; Mandal, S.; Gao, B.; Bolan, N.S.; and Ok, Y.S. (2016). Engineered/designer biochar for contaminant removal/immobilization from soil and water: Potential and implication of biochar modification. *Chemosphere*, 148, 276-291.

46. Ooi, C.-H.; Cheah, W.-K.; Sim, Y.-L.; Pung, S.-Y.; and Yeoh, F.-Y. (2017). Conversion and characterization of activated carbon fibre derived from palm empty fruit bunch waste and its kinetic study on urea adsorption. *Journal of Environmental Management*, 197, 199-205.

47. Jamari, S.S.; and Howse, J.R. (2012). The effect of the hydrothermal carbonization process on palm oil empty fruit bunch. *Biomass and Bioenergy*, 47, 82-90.

48. Yavari, S.; Malakahmad, A.; Sapari, N.B.; and Yavari, S. (2017). Synthesis optimization of oil palm empty fruit bunch and rice husk biochars for removal of imazapic and imazapyr herbicides. *Journal of Environmental Management*, 193, 201-210.

49. Komnitsas, K.A.; and Zaharaki, D. (2016). Morphology of modified biochar and its potential for phenol removal from aqueous solutions. *Frontiers in Environmental Science*, 4, Article 26, 11 pages.

50. Mahmood, W.M.F.W.; Ariffin, M.A.; Harun, Z.; Ishak, N.A.I.M.; Ghani, J.A.; and Rahman, M.N.A. (2015). Characterisation and potential use of biochar from gasified oil palm wastes. *Journal of Engineering Science and Technology (JESTEC)*, Special Issue on 4th International Technical Conference, 45-54.